Design of Low-bandwidth Spatially Distributed Feedback

Dimitry Gorinevsky, *Fellow, IEEE,* Stephen Boyd, *Fellow, IEEE,* and Gunter Stein *Fellow, IEEE,*

***Abstract*—The paper considers a family of linear time-invariant and spatially-invariant (LTSI) systems that are both distributed and localized. The spatial responses of the distributed plant are localized in spatial neighborhoods of each location. The feedback computations are also distributed and the information flow is localized in a spatial neighborhood of each location. The feedback is aimed at controlling spatial distributions of variables in the systems with a relatively low bandwidth in the time direction. Such systems have many important applications including industrial processes, imaging systems, signal and image processing, and others.**

We describe a new method for designing (tuning) a certain family of low-bandwidth controllers for such plants. We consider LTSI controllers with a fixed structure, which is PID or similar low-bandwidth feedback in time and local in spatial coordinates. Two spatial feedback filters, symmetric and with finite spatial response, modify the local PID control signal by mixing in the error and control signals at nearby nodes. These two filters provide loopshaping and regularization of the spatial feedback loop. Like an ordinary PID controller, this controller structure is simple, but provides adequate performance in many practical settings.

We cast a variety of specifications on the steady-state spatial response of the controller and its time response as a set of linear inequalities on the design variables, and so can carry out the design of the spatial filters using linear programming. The method handles steady-state limits on actuator signals, error signals, and several constraints related to robustness to plant and controller variation. The method allows handling the effects of boundary conditions and guaranteed closed-loop spatial or time decay. It does appear to work very well for low-bandwidth controllers, and so is applicable in a variety of practical situations.

***Index Terms*—Distributed system control, multidimensional, optimization, PID, bandwidth, loopshaping**

I. INTRODUCTION

THIS paper is on feedback control design in large distributed array systems. Array signal processing is a mature field with well understood design and analysis methods; there are numerous practical applications. Array control (array feedback) field is much less mature and is an emerging technology. We consider array systems with spatially distributed feedback.

Array control systems have been used in industrial processes for a long time. Perhaps the most widespread industrial application is in control of flat sheet processes, such as paper or plastic sheet manufacturing, where linear arrays of up to 300 actuators might be employed. Paper machine processes are very diverse. They use actuator arrays for boundary control of turbulent pulp flow, thermal profile control, moisture control, and other physical processes; see [23], [19], [32] and references there for more detail. The empirical models and problem statements used in industry for control of flat sheet processes do not depend on the underlying physics and closely resemble the formulation in this paper.

Other industrial applications of array control are related to thermal processing: in semiconductor manufacturing, crystal growing [1], and material heat processing. In these applications, spatial profiles of temperature are controlled using arrays of heating elements. An iterative learning control of batch thermal processing can also be described as a 2-D system (one coordinate is the local time in the batch and another the batch number) and leads to a closely related problem statement, see [16]. A cross-sample of industrial applications of distributed control including a few thermal processes can be found in [13].

In active or adaptive optics applications, large 2-D arrays of actuators deform a reflecting surface of a mirror to achieve wavefront control. A deformable mirror control analysis closely related to formulation in this paper is presented in [31] where further references can be found. A related area is shape control of large scale deformable reflectors for ground and space applications, e.g., see [22].

Future array control applications could rely on low-cost manufacturing of large arrays of actuators and sensors as Micro-Electro Mechanical Systems (MEMS). It might be possible to have computing embedded with the actuators. Several futuristic aerospace applications were discussed in the literature including micro-adaptive flow control using arrays of microactuators distributed over an airfoil or a channel boundary.

In addition to the mentioned control applications, distributed feedback is important in estimation problems. In systems theory, estimation is dual to control, hence, the similarity in the feedback analysis and design. The distributed estimation can be encountered in processing data described by a series of images, such as in video processing, medical image processing (computational tomography, MRI, ultrasound imaging, etc), remote earth observation, nondestructive evaluation of materials and structures, and more. The distributed estimation is closely related to solution of distributed inverse problems such as deblurring in image processing and grid methods for solving partial differential equations. Formulations of image processing and multidimensional filtering problem related to this paper and further references could be found in [17], [20].

In this paper we assume that the distributed arrays are large and make a regular spatial pattern. A fundamental technical approach to analysis of such systems is by assuming that the arrays have an infinite spatial extent (or are circulant). In that

D. Gorinevsky and S. Boyd are with Information Systems Lab, Stanford University, Stanford, CA 94305, USA, e-mail: gorin@stanford.edu; boyd@stanford.edu

G. Stein is with Honeywell Labs, Minneapolis, MN 55418, e-mail: GunterStein@aol.com

This work was in part supported by the NSF GOALI Grant ECS-0529426 and AFOSR grant FA9550-06-1-0514

case, an array can be modeled as a multidimensional system and analyzed by changing from spatial coordinates to spatial frequencies. Explanation and justification of spatial frequency transforms are available in many signal processing texts and papers including [4], [7] as well as in several image processing textbooks. A relatively recent control-oriented discussion can be found in [2]. If (closed-loop) responses decay fast enough spatially, an infinite-array multidimensional system model can be used with a finite array and boundary effects are limited. This is discussed further in more detail.

Modern control-theoretic approaches to analysis and design of feedback in large (or infinite) distributed systems with regular array structure were proposed and explored in a number of publications. The most relevant to this paper are [3], [10], [11], [12], [21], where further references can be found. Most of this work is focused on design of high-performance spatially invariant feedback control systems, with performance and robustness guarantees. Modern control design methods, such as linear matrix inequalities and mu-analysis are applied to the distributed systems

Practical use of advanced control-theoretic approaches is limited, even for usual lumped system. Herein, we pose less ambitious control-theoretical goals in the hope of developing methods that are easier to apply in practice; we focus on tuning methods for distributed generalizations of low bandwidth PID controllers. In practice, more than 90% of the control loops use PID, or PI, or PD, or P controllers. Since this is true for usual, lumped, systems there is a hope that a simple distributed generalization of a PID controller could satisfy the needs of most array feedback applications. Realization of this vision requires easily understood methods for controller tuning (design within the given simple structure).

Lumped systems with PID control usually have a decaying open-loop response. Less forgiving systems might require advanced control approaches, but are a minority in practice. We assume that a response of the distributed system decays in time and in space. This is the case in existing practical applications of array control. For such systems distributed PID-type control should be adequate.

There is substantial body of control-theoretical work analyzing PDE models. Our work has a different flavor. Industrial PID control design and tuning typically relies on basic models acquired in an simple identification test. Similarly, we describe a distributed system by an empirical spatial and time response; see [19] for an example of industrial application where such responses are directly identified. The PDE models might or might not be available.

In industrial array control (e.g., industrial cross-directional control of paper machines or temperature control), practitioners usually start from attempting decoupled zonal control. Each zone would include an actuator (or a few) and will be controlled independently of others. If there is a substantial interaction between the zones, this simple approach is not feasible. Spatial filtering of the feedback loop signals becomes necessary. This paper considers a loopshaping approach to selecting the spatial filters such that the performance, robustness, and other specifications are satisfied (if this is possible).

An approach closely related to ours, but less automated, is spatial loopshaping design (or tuning) of a distributed controller, as discussed in [32], [33]. The localized controller in [32], [33] is obtained by designing a non-localized controller, which is then truncated to provide a localized controller. Herein we assume a simple localized controller structure on the outset and develop a formal design method that allows accommodating many important engineering specifications for controller design.

Since the controller structure is assumed at the outset, the solution pursued in this work is not completely general. This enables us to achieve a rather complete solution of the problem.

In this paper, we consider a spatially distributed system analog of low-bandwidth PID control. A standard digital PID controller uses three values of the plant output (current, past and the integral) for computing the control. In a similar way, our 'spatial PID' controller uses data from a few neighboring array cells. Such control is relatively simple to implement computationally. For centralized implementation of the array control, simplifying computations needed for hundreds or thousands of actuators might be critical. The same algorithms can be conveniently implemented in an array of distributed embedded processors. Parallel processing makes computational performance less of an issue but constraints on communication between the processors become important; local communication with the nearest neighbors can be performed most efficiently, see [28].

Like an ordinary PID controller, the distributed controller structure considered in this paper, provides adequate performance in many, or even most, practical situations. This was demonstrated in a number of applications. Also like an ordinary PID controller, it is not meant to achieve a limit of possible performance; it is meant to be adequate, after proper tuning, in many practical cases.

An ordinary PID control implicitly assumes that the plant dynamics can be approximated as a first-order system. The proposed distributed controller is based on two such assumptions. First, that the space and time dynamics are separable. The second is that integrator dynamics are dominant in the closed loop.

The contribution of this paper is in formulating the spatially distributed controller design (tuning) problem as a convex optimization problem. Localized spatial (FIR) operators are assumed at the outset, and the main engineering specifications are accommodated within a linear programming (LP) optimization framework. This allows for a computationally efficient and conceptually clean one-shot solution for the optimal FIR weights in the controller. We show how formal specifications for performance, robustness, time decay, spatial decay, and some others closed-loop characteristics can be incorporated into such LP-based design.

We will see that the conversion of the problem to an LP is possible because the spatial responses considered are *symmetric*. This makes the spatial transfer functions (numerator and denominator) *real* and enables us to convert linear fractional (closed-loop) design constraints into linear constraints. The same trick does not work in the absence of symmetry.

The idea that symmetry of a pulse response leads to a real transfer function, and therefore limits on the frequency response can be expressed as linear inequalities, is not new; it is the basis of linear programming based design of symmetric FIR filters for signal processing applications, which has been done at least since 1969 (see [5, p. 380]). In this paper, however, we consider closed-loop expressions, which are *linear fractional* expressions in the FIR filter weights. The linear fractional expressions in filter design were cast as LP problems, e.g., see [8], [14], [30]. However, to the best of the authors' knowledge, this has not been done in a feedback control design context before.

II. Problem statement

Consider a distributed system consisting of an array of identical cells. For each cell there is a scalar control handle u and a scalar feedback measurement y. There is also interaction between the cells in the sense that will be explained further in the paper. Though there are several obvious ways to generalize the analysis and design of this paper to cells with multiple inputs and outputs, we assume SISO (single-input single output) cells for the sake of presentation clarity. Many practical applications, in particular all of the applications mentioned in Introduction involve arrays with SISO cells.

To explain the motivation for the system model and controller structure considered in this paper, we will introduce a series of increasingly complex models and controllers for such system. The models and controller structure choice are guided by engineering considerations auxiliary to mathematical analysis. At the same time, we present quite rigorous analysis and design of the control loop for the formulated equations.

A. SISO model

Let us start from the simplest model and control law. An approach that a practitioner would initially attempt using for an array system is to assume that there is no cross-cell interaction such that each cell can be controlled separately. The interaction is attributed to model uncertainty. The idea is that if the designed feedback loop is sufficiently robust, it would work as desired despite the presence of the spatial interaction.

If the cells are identical and do not interact, it is sufficient to consider a single cell. We assume that the output signal y of the cell is related to the control (input) signal u as

$$y \quad = \quad g(z^{-1})u + d, \tag{1}$$

where d is the disturbance input, z^{-1} is a unit delay operator and $g(z^{-1})$ can be both considered as a system discrete transfer function and a dynamical response operator.

We assume that a robust (low-bandwidth) feedback is used to control the output of the SISO loop (1) towards the setpoint y_d. The control law has the form

$$u \quad = \quad z^{-1}u - z^{-1}c(z^{-1})(y - y_d), \tag{2}$$

The controller $c(z^{-1})$ is in the velocity form to emphasize the presence of an integrator to counter slow changing and steady state disturbance. Practically used industrial controllers usually include an integrator as assumed in (2). This includes a PI or PID controller (considered in the examples examples of Section III-A and Section V), or a Dahlin controller (discrete-time Smith predictor), which is used in paper web manufacturing control. We assume that the plant response might be instantaneous, i.e., $g(z^{-1})$ in (1) is proper but might be not strictly proper. There is no feedthrough in the loop, however, and that is reflected by the unit delay operator z^{-1} shown at the feedback term in (2).

The closed loop transfer function representation of the system (1), (2) has the form

$$\begin{aligned} y \quad = \quad & \frac{z^{-1}c(z^{-1})}{1 - z^{-1} + z^{-1}c(z^{-1})g(z^{-1})} y_d \\ & + \frac{1 - z^{-1}}{1 - z^{-1} + z^{-1}c(z^{-1})g(z^{-1})} d \end{aligned} \tag{3}$$

In what follows, we assume that the closed loop transfer functions in (3) are stable and provide gain and phase margins to accommodate large uncertainty. Yet, in many practical applications the cell interaction is significant and cannot be simply attributed to the modeling uncertainty. More detailed modeling and control design aimed at such applications are presented below.

B. Separable two-dimensional plant model

In this paper, an array control system is modeled as a linear time-invariant spatially-invariant (LTSI) system. We assume that the array cells make a regular spatial pattern and that interaction between the neighboring cells repeats itself from cell to cell up to the respective spatial shift. A more in-depth description of LTSI control systems can be found in [2], [11]. An LTSI model allows for an efficient multidimensional frequency-domain analysis of the problem. The analysis involving spatial frequencies can be considered as modal analysis of the system dynamics, since the spatial sinusoids are the eigenmodes of a spatially invariant system [2].

An LTSI model does not consider boundary effects present in a finite array (unless it has a circulant structure). Boundary condition issues (which arise when the true plant and controller are not spatially infinite) can be integrated into the framework described herein as a deviation from the LTSI model, see [24], [26]. The boundary effects are closely related to the closed-loop spatial response decay, which is further considered as one of the important formal design specifications. Such handling of boundary conditions in Subsection 3.4 is in fact one of the major contributions of this paper.

Consider a two-dimensional (2-D) distributed system evolving in the integer time $t = 0, 1, \ldots$ and with an integer spatial coordinate $x = \ldots, -1, 0, 1, \ldots$ indexing the actuator cells. The (scalar) actuator or control signal will be denoted $u = u(t, x)$, which is the control applied by actuator number x in the array, at time t. The (scalar) process output is $y = y(t, x)$, where one measurement per actuator, and per time sample, is assumed. A general input-output model of an LTSI plant has the 2-D convolution form

$$y(t, x) = \sum_{k=0}^{\infty} \sum_{n=-\infty}^{\infty} h(t - k, x - n) u(k, n), \tag{4}$$

where $h(t,x)$ is the system 2-D impulse response function, or system Green's function.

We will assume a *separable* plant model, which has the form

$$h(t,x) = h_t(t)\ h_x(x), \tag{5}$$

where $h_t(t)$ is the plant time impulse response, and $h_x(x)$ is the plant spatial impulse response. We assume that h_t is causal, i.e., $h_t(t) = 0$ for $t < 0$. We will also assume that the plant is spatially symmetric, which means that $h_x(-x) = h_x(x)$. (The same methods work for plants that are spatially anti-symmetric, i.e., satisfy $h_x(-x) = -h_x(x)$.)

The analysis to follow uses a 2-D transfer function of the plant obtained by computing a z-transform of the pulse response (5). This transfer function has the form $H(z,\lambda) = g(z^{-1})G(\lambda)$, where $g(z^{-1})$ is the z-transform of the dynamical impulse response $h_t(t)$ in (5) and $G(\lambda)$ is a spatial transfer function computed as the (two-sided) z-transform of the spatial impulse response (Green function) $h_x(x)$. The plant is assumed stable and the spatial response absolutely summable (spatially stable). This means $g(z^{-1})$ is analytic inside the unit circle $|z| \le 1$ in the complex plane, and $G(\lambda)$ is analytic inside an annulus $r \le |\lambda| \le r^{-1}$, where $0 < r \le 1$.

The separable 2-D plant model is $y = g(z^{-1})G(\lambda)u$. In this model z^{-1} can be interpreted as a unit time delay operator and λ as a unit positive spatial displacement operator. We assume that g and G are scaled so $g(1) = 1$, i.e., the time transfer function g is normalized to have unit static gain. The assumed spatial symmetry implies that the spatial transfer function G is *real* for $|\lambda| = 1$. (If the plant were spatially anti-symmetric, then G would be pure imaginary for $|\lambda| = 1$.)

Separable models are applicable in many distributed systems where actuator dynamics or sensor dynamics or dynamics of a fixed dynamical filter are dominant. These dominant time dynamics are described by the time response $h_t(t)$ while $h_x(x)$ gives the steady-state spatial response shape. Models of the form (5) are used in many practical applications of array control discussed in Introduction.

A separable model (5) might be also obtained as an approximation of a general impulse response. As an example, consider a distributed system described by a heat equation

$$\frac{\partial^2 y}{\partial x^2} = \frac{\partial y}{\partial t} + ay + u, \tag{6}$$

where $x \in \Re$ is spatial coordinate, $t \in \Re^+$ is time, $y = y(t,x)$ is the temperature, $u = u(t,x)$ is the control input, and a is a thermal loss factor. The actuation and measurement are concentrated (as δ-functions) at integer coordinates. An input-output map of the system can be represented in the form (4) with the impulse response (Green function of (6)) being

$$h(t,x) = e^{-ta}(4\pi t)^{1/2}e^{-x^2/(4t)}, \tag{7}$$

where $t > 0$ and x are integers; we assume that there is a one sample delay between the measurement and control so that $h(t = 0, x) = 0$. We assume that $a > 0$, which means the system dissipates the heat and the impulse response (7) exponentially decays with time. This is the case for distributed heating control applications in papermaking, manufacturing, materials processing, and semiconductors.

The response (7) is not separable. Yet it can be approximated as such. Consider the argument domain $D_L = \{t, x : (t = 0, 1, \ldots, 2L+1;\ \ x = -L, \ldots, L)\}$. For large enough L, the impulse response is vanishingly small outside the domain D_L. Inside D_L, the values $h(t,x)$, $\{t,x\} \in D_L$ could be considered as entries of a matrix H_L. A singular value decomposition of H_L has the form

$$h(t,x) = \sum_{k=1}^{2L+1} g_k(t)\sigma_k h_k(x), \tag{8}$$

where $g_k(\cdot)$ and $h_k(\cdot)$ correspond to the left and right singular vectors of H_L respectively, and σ_k is the respective singular value. A separable model (5) can be obtained as a truncation of (8) with $h_t(t) = \sigma_1 g_1(t)$ and $h_x(x) = h_1(x)$. If the first singular value is much larger than the rest, the approximation is accurate. This holds in many applications.

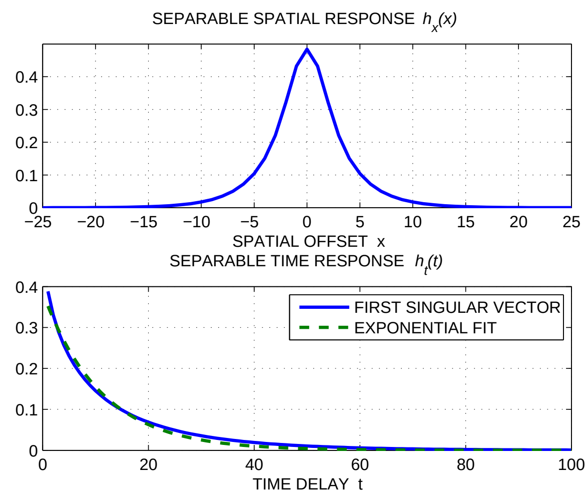

Fig. 1. Separable approximation of the heat equation response.

Assume $a = 0.05$ and $L = 25$. For the response (7) the first few singular values σ_k in (8) computed for the domain D_{25} are: 0.8668, 0.2636, 0.0931, 0.0341, 0.0126, 0.0046, 0.0016. The obtained spatial response $h_x(x) = \sigma_1 g_1(t)$ and time response $h_t(t) = h_1(x)$ of the separable approximation are shown in Figure 1 as solid lines. The dashed line in the lower plot is a least square fit of a first-order time response model (exponential response). An L_2 error for the separable approximation given by the ratio of the second and the first singular values is about 30%. However, as discussed further in the paper, an H_∞ approximation error (a maximal error magnitude over spatial and dynamical frequencies) is in fact important for the analysis. This error is just 22%, much smaller than the 33% H_∞ robustness specification implemented in the detailed design example of Section IV.

C. *Multidimensional model*

We will further consider a generalization of the just introduced separable model to a larger number of spatial dimensions.

Consider now a multidimensional system with n spatial coordinates and time. With some overload of notation denote the integer coordinate vector $x = [x_1 \ \ldots \ x_n]^T$. The cells in the n-D array have control inputs $u = u(t, x)$ and outputs $y = y(t, x)$. We assume that the system has a separable impulse response $h(t, x) = h_t(t)h_x(x)$ and introduce the spatial operator

$$G(\lambda) = \sum_{x_1=-\infty}^{\infty} \cdots \sum_{x_n=-\infty}^{\infty} \lambda_1^{x_1} \cdots \lambda_n^{x_n} h_x([x_1 \ \ldots x_n]^T), \quad (9)$$

where $\lambda = [\lambda_1 \ \ldots \ \lambda_n]^T$ is the vector of the Laplace indeterminates. As usual, an indeterminant λ_k can be interpreted as either complex variable or a unit shift operator for the spatial coordinate x_k. This should be clear from the context.

With an overload of notation, the plant model used in the control design and analysis has the form

$$y \quad = \quad g(z^{-1})G(\lambda)u + d, \quad (10)$$

where $d = d(x)$ is a static disturbance. The earlier considered 2-D model is a special case of the multidimensional model (10) for $n = 1$.

We assume that the system spatial response $h_x(x)$ is symmetric (or anti-symmetric) in each of the variables $x_1 \ \ldots x_n$, such that either $h_x([x_1 \ \ldots \ -x_k \ldots \ x_n]^T) = h_x([x_1 \ \ldots \ x_k \ldots \ x_n]^T)$ or $h_x([x_1 \ \ldots \ -x_k \ldots \ x_n]^T) = -h_x([x_1 \ \ldots \ x_k \ldots \ x_n]^T)$. Denote the spatial frequency vectors

$$\nu = [\nu_1 \ \ldots \ \nu_n]^T, \qquad e^{i\nu} = [e^{i\nu_1} \ \ldots \ e^{i\nu_n}]^T$$

The symmetry (anti-symmetry) assumption means that the non-causal transfer function $G(e^{iv})$ is real (or purely imaginary).

D. Control problem

We are interested in low-bandwidth control of the multidimensional plant (10). The goal is to cancel the steady-state error in reaching the desired spatial profile $y_d(x)$. The separable model (10) is an extension of (1). Consider now a separable controller that extends (2) in a similar way.

$$u = z^{-1}u - z^{-1}c(z^{-1})K(\lambda)(y - y_d), \quad (11)$$

where $c(z^{-1})$ describes the controller time-dynamics. The function of the spatial operator $K(\lambda)$ is to improve the closed-loop system response by compensating for the spatial interaction effects reflected by the operator $G(\lambda)$ in (10).

We now consider the closed-loop dynamics for the system (10)–(11). As discussed in more detail in [2], an LTSI system can be diagonalized by the spatial sinusoids. By substituting $\lambda = e^{i\nu}$ we obtain the modal dynamics for the spatial frequency ν. With some overload of notation, the control update dynamics for the mode at frequency ν are

$$\begin{aligned} zu(t, \nu) \quad &= \quad u(t, \nu) - K(e^{i\nu})G(e^{i\nu})g(z^{-1})c(z^{-1})u(t, \nu) \\ &\quad -K(e^{i\nu})c(z^{-1})[d(\nu) - y_d(\nu)], \end{aligned} \quad (12)$$

where $y_d(\nu)$ is a Fourier transform of $y_d(x)$

$$y_d(\nu) = (2\pi)^{-n} \sum_{x_1} \cdots \sum_{x_n} y_d(x) e^{i\nu_1 x_1} \ldots e^{i\nu_1 x_n},$$

and $d(\nu)$ is a Fourier transform of $d(x)$.

At high spatial frequencies, where $G(e^{iv}) \approx 0$, the actuation signal might experience unlimited growth. In control of industrial distributed processes, this effect is known as actuator picketing. To see this, suppose the plant gain $G(e^{i\nu})$ is zero at some spatial frequency ν. The dynamics (12) at this spatial frequency can be approximated as

$$zu(t, \nu) \quad = \quad u(t, \nu) - K(e^{i\nu})c(z^{-1})(d(\nu) - y_d(\nu)). (13)$$

The second term in the r.h.s. (13) does not depend on control u. However small the controller gain $K(e^{i\nu})$ is, the integrator in (13) will keep adding the error until the feedback signal becomes extremely large. The described situation is never encountered in ‘normal’ PID control. This is because the plant gain is always nonzero as a precondition of system design for implementation of closed-loop control. In a distributed system, plant gain might be zero for some modes while other modes are perfectly controllable.

The problem can be resolved by modifying the controller (11) for out-of-band control at frequencies where $|G(e^{i\nu})| \ll 1$. At these frequencies, the compensation of the error $y - y_d$ is not possible and the control convergence is most important. It can be achieved by using a controller structure given by

$$u = z^{-1}u - z^{-1}c(z^{-1})K(\lambda)(y - y_d) - z^{-1}S(\lambda)u \quad (14)$$

The first two terms in (14) have the same form as in (11). The third term introduces an additional degree of freedom for the and can be interpreted as a regularization term. The spatial operator $S(\lambda)$ introduces an integrator leakage term enforcing the out-of-band control convergence.

The regularization term is the best understood in relation to the system steady-state. It prevents an attempt to compensate an error at spatial frequencies where a small plant gain could lead to control inputs growing excessively large. This corresponds to a regularized inversion of an ill-defined plant [34]. Controllers of the form (14) have been used in web manufacturing processes [23], [15], [32].

We will assume that the controller, like the plant, is spatially symmetric, i.e., K and S are symmetric FIR filters; $K(\lambda)$ and $S(\lambda)$ are real for $|\lambda_1| = \ \ldots \ = |\lambda_n| = 1$. (For a plant where spatial response is anti-symmetric in some coordinates, we choose K anti-symmetric in the same coordinates and symmetric S.)

The main problem is to design the spatial operators $K(\lambda)$ and $S(\lambda)$. We assume that the spatial filters $K(\lambda)$ and $S(\lambda)$ are FIR operators, which implies that the controller (14) is spatially localized; the control signal $u(t, x)$ is computed based on only a finite number of error and actuator signals, at nearby actuator cells. This reflects important communication and computing constraints. For a centralized controller (finite but large array) FIR operators K and S can be implemented with high computational efficiency as convolution kernels applied to respective spatial variable profiles; for implementation through distributed embedded computing, K and S being FIR limits communication to a few near neighbors only.

The dynamical controller $c(z^{-1})$ in (14) (together with the integrator term) can be a simple low-bandwidth controller, such as a PI or PID controller. Using PI or PID controllers requires few assumptions about the plant. PID control can be made work and provides adequate performance for most practical problems. We can interpret the controller (14) as a simple LTSI generalization of the classical PID controller.

E. Estimation problem

Consider now a problem of estimating (filtering) the state of a multidimensional system. In systems theory, estimation is dual to control, hence, essentially the same mathematical approach can be used. The distributed estimation problem statement is a variation of the distributed control problem formulated above. The applications are in image deblurring, nondestructive evaluation of structural integrity, medical image processing, video processing, and scientific data processing.

Consider a problem of filtering a $(n+1)$-D signal, a time sequence of n-D images (data arrays) $y = y(t, x_1, \ldots, x_n)$. It is assumed that each observed image data array includes underlying data $v = v(t, x_1, \ldots, x_n)$ distorted by the observation method and an additive noise (disturbance) $d = d(t, x_1, \ldots, x_n)$. The image model has the form

$$y \;=\; G(\lambda)v + d, \tag{15}$$

where $G(\lambda)$ is the blur (distortion) operator and $\lambda = [\lambda_1 \; \ldots \; \lambda_n]^T$ is the unit spatial shift operator vector. The distortion can be caused by an off-focus camera in optical imaging, by Radon transform blur in the computed tomography, or other reasons. In what follows we assume that the distortion operator $G(\lambda)$ has some type of symmetry - the same assumption as in the control problem statement above. We assume that the underlying image v slowly evolves in time and the goal of the filtering is to estimate v despite the presence of the random disturbance d.

As a basis for model-based filter design, consider the following random walk model for the inderlying image data

$$v \;=\; z^{-1}v + \xi \tag{16}$$

where $\xi = \xi(t, x_1, \ldots, x_n)$ is a random driving noise sequence uncorrelated in time.

One way of designing a filter is to assume that d in (15) and ξ in (16) are independent Gaussian processes uncorrelated in time and with spatially invariant covariances independent of time. In that case, an optimal linear filter can be designed as a stationary Kalman Filter observer of the form

$$u = z^{-1}u + z^{-1}K(\lambda)(y - G(\lambda)u), \tag{17}$$

where the feedback operator $K(\lambda)$ can be obtained by solving an operator Riccati Equation, see [2].

An operator Riccati Equation for a multidimensional system is hard to solve in practice. Another problem is that the optimal feedback operator $K(\lambda)$ computed from a Riccati Equation has an infinite support and cannot be described by a rational transfer function. Therefore, a more practical solution is to design $K(\lambda)$ as an easy to implement FIR filter operator such that the filter has required performance. This is an approach pursued in this paper.

Whichever way $K(\lambda)$ is designed, the closed-loop dynamics for the distributed estimation update (15), (17) resemble those for the distributed control (10), (11) with $g(z^{-1}) = 1$ and $c(z^{-1}) = 1$ and with y instead of $d - y_d$. This leads to the same issue of error accumulation at high spatial frequencies (where $|G(e^{i\nu})| \ll 1$) as discussed for the distributed control problem. In the estimation problem, it is the estimation error $v - u$ that might grow unchecked. The approach to overcome this problem is to add a regularization term to the feedback update (17) in the form of an integrator leakage. This is implemented as an update of the form (14) with y instead of $d - y_d$.

$$u = z^{-1}u + z^{-1}K(\lambda)(y - \hat{y}) - S(\lambda)z^{-1}u, \quad \hat{y} = G(\lambda)u \tag{18}$$

In some cases, the input signal estimate u might be used as the filter output. In other cases, the prediction $\hat{y}$ is the filter output.

With the filter structure (18) fixed, the design problem is to find the FIR spatial operators $K(\lambda)$ and $S(\lambda)$ such that the filter performance, robustness, and other specifications are satisfied. This problem has the same form as the design of the operators $K(\lambda)$ and $S(\lambda)$ in (10), (14). Of course, the engineering specifications in the estimation problem would follow from different practical considerations than in the control problem. However, the general form of the specifications is the same and the same design and analysis approach can be used in both cases.

The remainder of the analysis and design in this paper is focused on the control problem implying that everything is applicable to the estimation problem as well, perhaps with a slight change. We return to the estimation problem in the example of Section V.

III. Control Design Specifications

We now consider the closed-loop dynamics for the system (10), (14). An LTSI system can be diagonalized by spatial sinusoids and we will perform the analysis and design in the spatial coordinate frequency domain. This section formulates many standard design specifications in the form of linear frequency depending inequalities. This lays foundation for the subsequent controller design approach.

A. Closed-loop dynamics

By substituting $\lambda_k = e^{i\nu_k}$ into (10), (14) we obtain the modal dynamics for the spatial frequency ν. With some overload of notation, the error dynamics for the mode at the frequency $\nu = [\nu_1 \; \ldots \; \nu_n]$ are

$$\begin{aligned} ze(t,\nu) \;&=\; (1 - s(\nu))e(t,\nu) \\ &\quad -l(\nu)g(z^{-1})c(z^{-1})e(t,\nu) + s(\nu)y_d(\nu), \end{aligned} \tag{19}$$

where $e(t,\nu) = y(t, e^{i\nu}) - y_d(\nu)$, and the modal loop gains are

$$l(\nu) = G(e^{i\nu})K(e^{i\nu}), \quad s(\nu) = S(e^{i\nu}) \tag{20}$$

Our assumptions of the spatial symmetry of the plant and controller imply that GK and S are real for $|\lambda_1| = \ldots = |\lambda_n| = 1$, so the modal loop gain $l(\nu)$ and the modal smoothing gain $s(\nu)$ in (19) are real numbers. More detail on the symmetry types is presented in Section V.

The equation (19) gives another interpretation of our basic controller structure: it can be considered as a family of independent PID (or other simple structure) controllers, one for each spatial frequency. The modal loop gain $l(\nu)$ and the modal smoothing gain $s(\nu)$ are determined by the coefficients of the spatial filters K and S. The tuning of these filters can be interpreted as the problem of tuning a *family* of the controllers, indexed by the spatial frequency vector ν.

Assume first that $s(\nu) = 0$. The modal error e will converge to zero provided that the loop gain $l > 0$ is sufficiently small and the steady-state gain of dynamical controller is such that $g(1)c(1) > 0$. The steady-state error in e is eliminated because of the integrator (a pole at z=1) present in the controller (14) for $S = 0$. The modal convergence can be made faster by increasing the loop gain l within certain limits. This is a usual loopshaping arrangement. The details of tuning the integrator gain, depend on the plant transfer function $g(z^{-1})$ and controller transfer function $c(z^{-1})$.

The operator S (and the gain $s(\nu)$) has an effect of regularizing the ill-defined problem of controlling a distributed plant with some zero modal gains. It can be called a 'smoothing' operator because small gain is usually associated with high spatial frequencies and the regularization has an effect of reducing the large amplitude of high frequency components in the control signal u.

For given plant response dynamics $g(z^{-1})$ and the dynamical controller $c(z^{-1})$, the closed-loop dynamics (19) are fully described by the two real gains l and s in (20). For given l, s, the dynamics do not depend on the plant spatial operator $G(\lambda)$.

Consider now a suitable loop performance index $J_p = J_p(l, s)$. One such simple index can be given by the closed loop convergence rate

$$J_p(l, s) = \max_k |z_k|, \tag{21}$$

where z_k are the system poles - the roots of the characteristic equation for (19)

$$1 - z^{-1} + lz^{-1}g(z^{-1})c(z^{-1}) + sz^{-1} = 0.$$

The performance specification for the controller design can be expressed in the form

$$\{l, s\} \in \mathcal{D}_p(\alpha), \qquad \mathcal{D}_p(\alpha) \equiv \{l, s : \; J_p(l, s) \leq \alpha\} \tag{22}$$

The performance index (21) can be computed numerically on a two-dimensional grid of the gains $\{l, s\}$. From that, using standard software, one can obtain the contour lines describing the boundary of the domain $\mathcal{D}_p(\alpha)$. Thus, the specification $\{l, s\} \in \mathcal{D}_p(\alpha)$ can be incorporated into the controller design framework.

In what follows, we use a convex approximation of the domain $\mathcal{D}_p(\alpha)$ by inscribing convex polygons inside this domains and expressing the domain as the linear inequalities of the form

$$\alpha_p l + \beta_p s \leq \gamma_p \tag{23}$$

where $\alpha_p, \beta_p, \gamma_p \in \Re^{N_p}$ express the polygon approximating $\mathcal{D}_p(\alpha)$. The inequalities (23), should be interpreted component-wise.

There can be several performance requirements of the form (22), such as feedback loop convergence, limited peaking of the loop response, rejection of dynamic disturbances, etc. The requirements can be also separately formulated for in-band and out-of-band spatial frequencies. The acceptable performance domain for each requirement can be similarly approximated by an inscribed polygon of the form (23). Combining the linear inequality sets of the form (23) for each of the requirements would yield a larger set of linear inequalities that still has the form (23) and is compatible with the design approach described below.

The domain $\mathcal{D}_p(\alpha)$ and its approximation (23) depend on the plant dynamics $g(z^{-1}) = 1$, controller $c(z^{-1}) = 1$ and the specific chosen performance index. To illustrate validity of the polygonal approximation of the domain $\mathcal{D}_p(\alpha)$ consider two commonly encountered examples of the dynamics.

Example 1: Simple delay feedback: Assume that $g(z^{-1}) = 1$ and $c(z^{-1}) = 1$. Such simple response with no dynamics is encountered in estimation problem and many practical distributed control problems where sampling time is much larger than the plant settling time. For this system, the single closed loop pole is real and the performance index (21) is $J_p(l, s) = |1 - l - s|$. In that case the domain (22) is $\mathcal{D}_p(\alpha) \equiv \{l, s : \; |1 - l - s| \leq \alpha\}$. It can be exactly expressed in the form (23), where

$$\alpha_p = \begin{bmatrix} -1 \\ 1 \end{bmatrix}, \;\; \beta_p = \begin{bmatrix} -1 \\ 1 \end{bmatrix}, \;\; \gamma_p = \begin{bmatrix} \alpha - 1 \\ \alpha + 1 \end{bmatrix}, \tag{24}$$

Example 2: First order system with PI control: Consider now a system with a first order dynamical response $g(z^{-1})$ and a PI controller. Assume that

$$g(z^{-1}) = \frac{z^{-1}}{1 - \tau z^{-1}} \tag{25}$$

$$c(z^{-1}) = k_P(1 - z^{-1}) + k_I \tag{26}$$

where $\tau = 0.8$, $k_P = 0.25$, and $k_I = 0.1$.

In that case the domain (22) $\mathcal{D}_p(\alpha)$ is shown in Figure 2. As an example of polygonal approximation, Figure 2 shows a polygonal approximation of the domain $\mathcal{D}_p(0.9)$ (dashed lines). This approximation can be expressed the inequalities of the form (23), where

$$\alpha_p = \begin{bmatrix} 1.45 \\ 1 \\ -0.45 \\ 0 \end{bmatrix}, \;\; \beta_p = \begin{bmatrix} 0 \\ 0 \\ -0.98 \\ -1.25 \end{bmatrix}, \;\; \gamma_p = \begin{bmatrix} -2.94 \\ 0.2 \\ 0.15 \\ -0.25 \end{bmatrix} \tag{27}$$

B. Steady-state performance specifications

The goal of this paper is to formulate an optimization approach to tuning the spatial FIR operators K and S in the controller (11). The main emphasis is on low-bandwidth control that is related to steady-state closed-loop response, i.e., the response for $z = 1$. By combining (10) and (11) the closed-loop spatial transfer functions can be obtained. The error $e = y - y_d$ and control u in steady-state (i.e.,

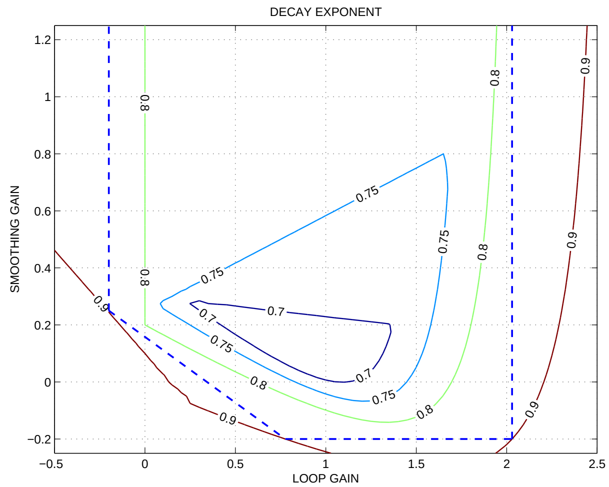

Fig. 2. Performance domain for PID control of a first-order system: the decay rate index.

at $z = 1$), and at spatial frequency $\nu = [\nu_1 \ \dots \ \nu_n]^T$ ($\lambda = e^{i\nu} = [e^{i\nu_1} \ \dots \ e^{i\nu_n}]^T$), are given by

$$e = \frac{S(e^{i\nu})}{S(e^{i\nu}) + G(e^{i\nu})k_I K(e^{i\nu})} y_d(\nu), \qquad (28)$$

$$u = \frac{k_I K(e^{i\nu})}{S(e^{i\nu}) + G(e^{i\nu})k_I K(e^{i\nu})} y_d(\nu), \qquad (29)$$

where the integrator gain is $k_I = c(1)$. Recall that $g(1) = 1$ is assumed.

For deriving engineering specifications on the control it will be assumed that a bound on the target profile y_d is available in the form $|y_d(\nu)| \leq d_0$, i.e., we have a known bound on the maximum of the of the target profile at every frequency. We require that for any such target profile, the magnitude of the control is bounded for all spatial frequencies, i.e., $|u| \leq u_0$) for all $\nu \in [0, 2\pi]^n$. Using (29), the last condition can be expressed in the form

$$\left| \frac{k_I K(e^{i\nu})}{S(e^{i\nu}) + G(e^{i\nu})k_I K(e^{i\nu})} \right| \leq u_0/d_0, \quad \text{for all } \nu. \qquad (30)$$

In a similar way we require that the magnitude of the steady-state error is bounded, i.e., $|e| \leq e_0$ for all ν in the band of spatial frequencies $\mathcal{B} \subseteq [0, \pi]^n$ over which we require good control performance. This leads to the steady-state performance condition

$$\left| \frac{S(e^{i\nu})}{S(e^{i\nu}) + G(e^{i\nu})k_I K(e^{i\nu})} \right| \leq e_0/d_0, \quad \text{for all } \nu \in \mathcal{B}. \qquad (31)$$

Unlike (30), which is required to hold for any spatial frequency ν, the small steady-state error condition (31) is required only within the spatial bandwidth of the system, $\nu \in \mathcal{B}$. This bandwidth might be taken, for example, as the set of the spatial frequencies where the plant gain is sufficiently large to ensure that the disturbances can be compensated without an excessive control effort, i.e., $\left\{ \nu \in \mathcal{B} : \ |K(e^{i\nu})| \geq k_0 \right\}$.

Since the bandwidth needs to be defined *before* the feedback operator K can be found, a more practical definition can be based on the knowledge that $k_I K(e^{i\nu}) G(e^{i\nu}) \approx 1$ in-band. Thus, the bandwidth domain can be defined as $\left\{ \nu \in \mathcal{B} : \ |G(e^{i\nu})| \leq g_0 \right\}$, where $g_0 = (k_I k_0)^{-1}$.

C. Steady-state robustness specifications

Another important engineering requirement is the robustness of the closed-loop system to plant modeling error. Assume that instead of the plant description (10), we have the following perturbed plant,

$$y = g(z^{-1})G(\lambda)u + \delta P(z^{-1}, \lambda)u, \qquad (32)$$

where $|\delta P| \leq \delta_0$ for $|z| \leq 1$, $|\lambda_1| = \ldots = |\lambda_n| = 1$. The small gain theorem guarantees stability of the closed-loop system with perturbed plant (32), and the controller (11), provided

$$\left| \frac{c(z^{-1})K(\lambda)}{1 - z^{-1} + z^{-1}S(\lambda) + z^{-1}c(z^{-1})g(z^{-1})G(\lambda)K(\lambda)} \right| \delta_0 < 1 \quad \text{for } |z| = 1, |\lambda_1| = \ldots = |\lambda_n| = 1. \qquad (33)$$

Since in low-bandwidth control the main control action takes place at low dynamical frequencies, a steady-state robustness condition will be considered in place of (33). For $|z| = 1$, (33) reduces to

$$\left| \frac{k_I K(\lambda)}{S(\lambda) + k_I G(\lambda) K(\lambda)} \right| \delta_0 < 1 \quad \text{for } |\lambda_1| = \ldots = |\lambda_n| = 1. \qquad (34)$$

We can also consider robustness to controller variations. A distributed controller implementation might differ from the designed controller, for several reasons: our analysis does not take boundary effects into account; and we may have sensor, actuator, or computing element faults in the distributed control system. Assume that instead of the nominal controller (11), we have

$$u = z^{-1}u - c(z^{-1})K(\lambda)(y - y_d) - z^{-1}S(\lambda)u + \delta C(z^{-1}, \lambda)u, \qquad (35)$$

where $|\delta C| \leq \delta_C$ for $|z| \leq 1$, $|\lambda_1| = \ldots = |\lambda_n| = 1$. Similar to how (34) is derived, the small-gain based steady-state robustness condition can be expressed in the form

$$\left| \frac{S(\lambda)}{S(\lambda) + k_I G(\lambda) K(\lambda)} \right| \delta_C < 1 \quad \text{for } |\lambda_1| = \ldots = |\lambda_n| = 1. \qquad (36)$$

Note that the robustness conditions (34), (36) are homogeneous in the operators S and K. There is a need to include one more, nonhomogeneous condition. The integrator in the controller might be implemented with an error because of the boundaries and potential faults as mentioned above. A very small error in the integrator might results in an instability if $K = 0$ and $S = 0$. This possibility is not covered by the homogeneous robustness condition (36).

Consider robustness to variations in the smoothing operator S. Assume that in (11) the smoothing operator is $S(\lambda) + \delta S(z^{-1}, \lambda)$, where $|\delta S(z^{-1}, \lambda)| \leq \delta_S$ for $|z| \leq 1$, $|\lambda_1| = \ldots = |\lambda_n| = 1$. Once again, we can derive a small-gain based robustness condition:

$$\left| \frac{1}{S(\lambda) + k_I G(\lambda) K(\lambda)} \right| \delta_S < 1 \quad \text{for } |\lambda_1| = \ldots = |\lambda_n| = 1. \qquad (37)$$

D. Spatial response decay

Consider now the design requirement related to the boundary condition influence. It can be demonstrated that this influence is limited by the characteristic width of the system impulse response. The emphasis of other design requirements considered above is on the steady-state closed-loop behavior. Similar to that, we consider the characteristic width of the steady-state closed-loop impulse response.

The impulse response is defined by a multivariable transfer function of the form (9) and has the same form as the respective transfer function. The previous subsections consider several steady-state transfer functions. For all of these, a steady state impulse response is described as

$$h(\lambda) = \frac{A(\lambda)}{B(\lambda)}, \quad B(\lambda) = S(\lambda) + k_I G(\lambda) K(\lambda), \tag{38}$$

where the denominator is same for all the steady-state loop transfer functions. The numerator $A(\lambda)$ depends on which impulse response is considered. For control response to disturbance, $A(\lambda) = k_I K(\lambda)$, while for the error response to disturbance, $A(\lambda) = S(\lambda)$. In the rest of this section, we assume that $B(\lambda)$ is a FIR operator. The feedback operators $S(\lambda)$ and $K(\lambda)$ are FIR. The plant spatial response $G(\lambda)$ can be modeled or approximated as FIR in most practical cases. We assume that N_B is the width of the FIR operator $B(\lambda)$, such that each of the n indexes of a nonzero element in $B(\lambda)$ does not exceed N_B.

Herein we will evaluate the impulse response width through its decay rate. The requirement is that the impulse response decays at least as fast as $r^{|k|}$, where k is the distance from the impulse and r is a design parameter, $0 < r < 1$. This response decay ensures that boundary condition influence is limited to a boundary layer with a characteristic width

$$L_b = N_A - 1/\log r \tag{39}$$

where N_A is the width of the FIR operator $A(\lambda)$. An impulse response having a decay exponent r requires that the transfer function $A(\lambda)/B(\lambda)$ is analytical in the n-D annulus domain

$$\lambda = [\lambda_1 \ \ldots \ \lambda_n]^T, \ \ r \le |\lambda_k| \le r^{-1}, \ \ r < 1, \tag{40}$$

Technical background on 2-sided z-transform leading to (40) can be found in [27]. The transfer function analyticity means that $B(\lambda)$ should not have zeros in the ring (40). Unfortunately this is a nonconvex constraint and it cannot be handled in a computationally efficient way. Instead, consider a convex constraint that conveniently enforces the spatial converegence and will be further shown to be a relaxation of $B(\lambda)$ not having zeros in the ring (40). This constraint has the form

$$|1 - B(e^{i\nu})| \le t < 1 \tag{41}$$

Recall that according to the made symmetry assumptions the frequency response $B(e^{i\nu}) = S(e^{iv}) + k_I G(e^{iv}) K(e^{iv})$ is real (or purely imaginary). The condition $B(e^{i\nu}) > 0$ is necessary for the input-output stability of the transfer function; otherwise the harmonics with frequency v where $B(e^{i\nu}) = 0$ will have an infinite amplification gain. This condition is discussed in [27] for one spatial variable. Assume now that $t = 0$. Then $B(\lambda) \equiv 1$ and we got an FIR filter with the transfer function $A(\lambda)$. The impulse response of the FIR filter is identically zero outside of the FIR filter support.

Consider a general case of $0 < t < 1$. One can show that smaller t in (41) guarantees faster decay of the filter impulse response. The following proposition holds

Proposition 1: Consider an IIR n-D filter $\frac{A(\lambda)}{B(\lambda)}$ (38), where a N_B-tap delay symmetric denominator $B(\lambda)$ satisfies (41). Then the impulse response $h(k_1, \ \ldots, k_n)$ of the IIR filter decays as

$$|h(k_1, \ \ldots, k_n)| \le c \cdot r^{\min[|k_1|, \ \ldots, |k_n|]}, \qquad r = t^{1/N_B}, \tag{42}$$

where c is a constant; $r = t^{1/N_B} < 1$ is the same as in (40); and the boundary layer width estimate (39) is $L_b = N_A - N_B/\log t$.

Proof: It is sufficient to prove (42) for the filter $1/B(\lambda)$, since a cascade FIR filter $A(\lambda)$ does not change the response decay rate. We will prove the following inequality equivalent to (42)

$$|h(k_1, \ldots, k_n)| \le \frac{t^{-n}}{1-t}, \text{ for } \max[|k_1|, \ldots, |k_n|] \ge n \cdot N_B \tag{43}$$

Denote $C(\lambda) = 1 - B(\lambda)$. For any $n > 1$

$$\begin{aligned} \frac{1}{B(\lambda)} &\equiv \frac{1}{1 - C(\lambda)} \\ &= \left[1 + C(\lambda) + \ldots + C^{n-1}(\lambda)\right] + \frac{C^n(\lambda)}{1 - C(\lambda)} \end{aligned} \tag{44}$$

The first n terms in the square brackets in the r.h.s. (44) describe an FIR filter with the width $(n-1)N_B$. The impulse response of this FIR filter is zero for $\max[|k_1|, \ \ldots, |k_n|] \ge n \cdot N_B$. For $\max[|k_1|, \ \ldots, |k_n|] \ge n \cdot N_B$, using the inverse Fourier transform to evaluate the impulse response $h(k_1, \ \ldots, k_n)$ yields

$$\begin{aligned} h(k_1, \ \ldots, k_n) &= \\ &\frac{1}{(2\pi)^n} \underbrace{\int_0^{2\pi} \cdots \int_0^{2\pi}}_{n} \frac{1}{B(e^{i\nu})} e^{-ik_1\nu_1} \cdots e^{-ik_n\nu_n} d\nu_1 \cdots d\nu_n \\ &= \frac{1}{(2\pi)^n} \underbrace{\int_0^{2\pi} \cdots \int_0^{2\pi}}_{n} \frac{C^n(e^{i\nu})}{1 - C(e^{i\nu})} e^{-ik^T\nu} d\nu \end{aligned} \tag{45}$$

In accordance with (41), $|C(e^{i\nu})| \le t < 1$. Hence, $\left|\frac{C^n(e^{i\nu})}{1-C(e^{i\nu})}\right| \le \frac{t^n}{1-t}$ and (43) follows immediately. Q.E.D.

E. Specification summary

In summary, the specifications are given by the loop-gain limit for dynamic stability (14), and

- the actuator limit (30)
- the performance specification (31)
- robustness to plant variation (34)
- robustness to controller variation (36)
- robustness to smoothing operator variation (37).
- performance specifications (23)
- spatial decay specifications (41)

Since the loop gain $l(\nu)$ is a linear function of $K(\nu)$ and the smoothing gain $s(\nu)$ is a linear function of $S(\nu)$ the feedback gain constraints (23), are linear in K and S for each frequency ν. Each of the other specifications has the form of a limit on the magnitude of a linear fractional function of $K(\lambda)$ and $S(\lambda)$, for all $|\lambda_1| = \ldots = |\lambda_n| = 1$, or (in the case of the performance specification) for some $|\lambda_1| = \ldots = |\lambda_n| = 1$.

IV. Optimization formulation

We now show how the design of the spatial filters K and S can be cast as a semi-infinite convex optimization problem, which can be approximated well as a linear program (and therefore solved efficiently). As briefly mentioned in Section III, these operators are constrained to be FIR operators such that information from near neighbors only is used when computing control at a particular spatial location. See [6] for a discussion of advantages to the convex optimization formulation.

A. Symmetry and realness

Recall that we assume that the plant spatial response operator $G(\lambda)$ is symmetric, such that $G(e^{i\nu})$ is real. We assume that the feedback operators $K(\lambda)$ and $S(\lambda)$ are symmetric too. Alternatively, the approach described below is applicable when $G(\lambda)$ is symmetric for some coordinates and anti-symmetric for other. In that case we assume that $K(\lambda)$ pocesses the same symmetry such that the frequency response $K(e^{i\nu})G(e^{i\nu})$ is real.

To provide a deeper insight into the operator symmetry and a background for the technical approach formulation, let us consider several types of symmetry.

1-D case: Let us start from the case of one spatial variable, when λ is a scalar. In the case when the FIR operator K is symmetric (which we assume when G is symmetric), we can express it as

$$K(\lambda) = \kappa_0 + \sum_{k=1}^{N} (\lambda^k + \lambda^{-k})\kappa_k, \tag{46}$$

where $\kappa_0, \ldots, \kappa_N$ are the coefficients. When $G(\lambda)$ is anti-symmetric, we take K to be anti-symmetric as well, in which case it has the form

$$K(\lambda) = \sum_{k=1}^{N} (\lambda^k - \lambda^{-k})\kappa_k. \tag{47}$$

(We will explain the method assuming that K and G are symmetric.) The smoothing FIR operator $S(\lambda)$ is always assumed to be symmetric, and has the form

$$S(\lambda) = \sigma_0 + \sum_{k=1}^{N} (\lambda^k + \lambda^{-k})\sigma_k, \tag{48}$$

where $\sigma_0, \ldots . \sigma_N$ are the coefficients. At the spatial frequency ν, i.e., $\lambda = e^{i\nu}$, we have

$$K = \kappa_0 + 2\sum_{k=1}^{N} \kappa_k \cos(k\nu), \quad S = \sigma_0 + 2\sum_{k=1}^{N} \sigma_k \cos(k\nu). \tag{49}$$

Let $x \in \mathbf{R}^{2N+2}$ be the vector of all the coefficients, i.e., our optimization variables:

$$x = [\kappa_0 \ \cdots \ \kappa_N \ \sigma_0 \ \cdots \ \sigma_N]^T. \tag{50}$$

For each spatial frequency ν, K and S are linear functions of x, and therefore so are the loop and smoothing gains, $l(\nu)$ and $s(\nu)$.

2-D symmetries: Let us discuss the symmetry patterns for a 2-D operator

$$B(\lambda) = B(\lambda_1, \lambda_2) = \sum_{m=1}^{M} \sum_{n=1}^{M} b_{m,n} \lambda_1^m \lambda_2^n$$

This operator could correspond to either of the two FIR feedback operators $K(\lambda)$ or $S(\lambda)$. The types of symmetry usually considered for 2-D filters include (see [25])

- 2-fold symmetry: $b_{m,n} = b_{-m,-n}$
- 4-fold symmetry: $b_{m,n} = b_{-m,-n} = b_{-m,n} = b_{m,-n}$
- 8-fold symmetry: $b_{m,n} = b_{-m,-n} = b_{-m,n} = b_{m,-n} = b_{n,m} = b_{-n,-m} = b_{-n,m} = b_{n,-m}$

In all of the above symmetry cases the operator $B(\lambda)$ can be expanded in the form similar to (46)–(48)

$$B(\lambda_1, \lambda_2) \quad = \quad \sum_{m=0}^{M_b} b_m P_m^M(\lambda_1, \lambda_2), \tag{51}$$

where $P_m^M(\lambda_1, \lambda_2)$ are the elementary polynomials defining the symmetry. The expansion (51) explicitly shows $M_b + 1$ independent filter design parameters b_m for the assumed symmetry type.

For 2-fold symmetry, the symmetric expansion polynomials can be expressed in the form

$$\begin{aligned} P_0^M(\lambda_1, \lambda_2) &= 1, \\ P_j^M(\lambda_1, \lambda_2) &= \lambda_2^j + \lambda_2^{-j}, \ \ (j = 1, \ldots, M), \\ P_{M+k}^M(\lambda_1, \lambda_2) &= \lambda_1^{l_k} \lambda_2^{m_k} + \lambda_1^{-l_k} \lambda_2^{-m_k}, \end{aligned} \tag{52}$$

where in the last line $1 \le l_k \le M$, $-M \le m_k \le M$ and $k = 1, \ldots, M(2M+1)$. The expansion size is $M_b = 1 + M + M(2M+1)$.

For 4-fold symmetry

$$\begin{aligned} \lambda P_0^M(\lambda_1, \lambda_2) &= 1, \\ P_j^M(\lambda_1, \lambda_2) &= \lambda_1^j + \lambda_1^{-j} + \lambda_2^j + \lambda_2^{-j}, \ \ (j = 1, \ldots, M), \\ P_{M+k}^M(\lambda_1, \lambda_2) &= \lambda_1^{l_k} \lambda_2^{m_k} + \lambda_1^{l_k} \lambda_2^{-m_k} \\ &\quad + \lambda_1^{-l_k} \lambda_2^{m_k} + \lambda_1^{-m_k} \lambda_2^{-l_k}, \end{aligned} \tag{53}$$

where in the last line $1 \le l_k \le M$, $1 \le m_k \le M$, and $k = 1, \ldots, M^2$. The expansion size is $M_b + 1 = 1 + M + M^2$.

For 8-fold symmetry

$$\begin{aligned} P_0^M(\lambda_1, \lambda_2) &= 1, \\ P_j^M(\lambda_1, \lambda_2) &= \lambda_1^j + \lambda_1^{-j} + \lambda_2^j + \lambda_2^{-j}, \\ P_{M+j}^M(\lambda_1, \lambda_2) &= \lambda_1^j \lambda_2^j + \lambda_1^{-j} \lambda_2^j \\ &\quad + \lambda_1^j \lambda_2^{-j} + \lambda_1^{-j} \lambda_2^{-j}, \\ P_{2M+k}^M(\lambda_1, \lambda_2) &= \lambda_1^{l_k} \lambda_2^{m_k} + \lambda_1^{l_k} \lambda_2^{-m_k} + \ \lambda_1^{-l_k} \lambda_2^{m_k} \\ &\quad + \lambda_1^{-l_k} \lambda_2^{-m_k} + \lambda_1^{m_k} \lambda_2^{l_k} + \lambda_1^{m_k} \lambda_2^{-l_k} \\ &\quad + \lambda_1^{-m_k} \lambda_2^{l_k} + \lambda_1^{-m_k} \lambda_2^{-l_k}, \end{aligned} \tag{54}$$

where $j = 1, \ldots, M$; in the last equation $1 \le l_k \le m_k - 1$, $2 \le m_k \le M$, and $k = 1, \ldots, M(M-1)/2$. The expansion size is $M_b + 1 = 1 + 2M + M(M-1)/2$.

Choosing a higher type of symmetry reduces the number of filter design parameters and is desirable where the symmetry of the requirements exists. To obtain frequency responses in (51)–(54), substitute $\lambda_1 = e^{iv_1}$ and $\lambda_2 = e^{iv_2}$. Because of the symmetry, the imaginary parts cancel and the real expansion functions $P_m^M(e^{iw_1}, e^{iw_2})$ are combinations of the frequency cosines.

In all of the considered symmetry cases, the frequency responses for the FIR feedback operators K and S in the controller (11) can be expressed in the same general form

$$\begin{aligned} K(e^{i\nu_1}, e^{i\nu_2}) &= c_K^T(e^{i\nu_1}, e^{i\nu_2}) p_K, \\ S(e^{i\nu_1}, e^{i\nu_2}) &= c_S^T(e^{i\nu_1}, e^{i\nu_2}) p_S, \qquad (55) \\ c_K(e^{i\nu_1}, e^{i\nu_2}) &= [P_0^M(e^{i\nu_1}, e^{i\nu_2}) \ldots P_{M_b}^M(e^{i\nu_1}, e^{i\nu_2})]^T, \\ p_K &= [\kappa_0 \ \kappa_1 \ \ldots \ \kappa_{M_b}]^T, \qquad (56) \\ c_S(e^{i\nu_1}, e^{i\nu_2}) &= [P_0^M(e^{i\nu_1}, e^{i\nu_2}) \ldots P_{M_b}^M(e^{i\nu_1}, e^{i\nu_2})]^T, \\ p_S &= [\sigma_0 \ \sigma_1 \ \ldots \ \sigma_{M_b}]^T, \qquad (57) \end{aligned}$$

Let $x \in \mathbf{R}^{2M_b+2}$ be the vector of all the coefficients, i.e., our optimization variables:

$$x = [\kappa_0 \ \cdots \ \kappa_N \ \sigma_0 \ \cdots \ \sigma_N]^T. \qquad (58)$$

For each spatial frequency ν, K and S are linear functions of x, and therefore so are the loop and smoothing gains, $l(\nu)$ and $s(\nu)$.

Other symmetries: One additional type of symmetry for 2-D array is hexagonal symmetry. Hexagonal actuator arrays are commonly used in adaptive optics where several thousand actuators might be used to control surface of a deformable mirror. A distributed control application with a hexagonal symmetry is considered in [31].

Some 3-D and 4-D applications of distributed feedback control exist on the estimation side, such as computational tomography or time-space filtering. A discussion of the filter symmetry types for such systems can be found in [29], [9].

The design and implementation approaches presented herein are directly applicable to higher-dimensional IIR filters. The only difference in the formulation is in the number of the independent coordinate arguments. The only difference in the computational design and implementation methods is in the potentially larger number of the points in a multidimensional frequency grid.

One more extension of the presented approach is to the case where $G(\lambda)$ is not symmetric. In that case the system can be 'squared down' by multiplying the plant output y in (10) by the conjugated operator $G^*(\lambda)$. This yields the system of the same form (10) with a symmetric spatial response $G^*(\lambda)G(\lambda)$. The 'squaring down' is especially efficient if G is a FIR operator.

B. Optimization problem

We will now show how all of the tuning specifications can be expressed as (infinite) sets of linear inequalities on the variable x (58). The operators K, and S, as well as the loop gain GK are linear in the tuning weights (components of the vector x. Therefore the following representation is possible

$$\begin{aligned} K(e^{i\nu}) = \bar{K}(\nu)^T x, \quad S(e^{i\nu}) &= \bar{S}(\nu)^T x, \\ k_I G(e^{i\nu}) K(e^{i\nu}) &= \bar{H}(\nu)^T x, \qquad (59) \end{aligned}$$

where $\bar{K}(\nu)$, $\bar{S}(\nu)$, and $\bar{H}(\nu)$ are column vectors with real components.

Expressing the constraints which involve linear fractional functions as linear constraints is not as straightforward. For each spatial frequency ν, the requirements (30), (31), (34), (36), and (37) have the form

$$\left| \frac{a^T x + b}{s(\nu) + k_I l(\nu)} \right| \le 1, \qquad (60)$$

where $a \in \mathbf{R}^{2M_b+2}$ and $b \in \mathbf{R}$ (and depend on the spatial frequencies, and also which specification is being represented).

Both the numerator and denominator in this equality are transformation of the operators K and S, which are in turn linear in the tuning parameters κ_k and σ_l in (46), (47), (48). In all cases the denominator is

$$S(e^{i\nu}) + k_I G(e^{i\nu}) K(e^{i\nu}) \qquad (61)$$

The second term in the denominator, $k_I l(\nu)$, is nonnegative, and is positive except at spatial frequencies where the plant gain is zero. In fact, the whole denominator must be positive at all spatial frequencies; indeed, the whole point of the smoothing operator S is to ensure $s(\nu) > 0$ for spatial frequencies where $l(\nu)$ is small. We can argue this as follows. Suppose the denominator (which is real) changes sign, and therefore is zero at some spatial frequency ν. At that frequency, the robustness to smoothing operator variation constraint, (37), is violated, since the numerator of the relevant transfer function is a nonzero constant, and the denominator vanishes, so the relevant transfer function is infinite (and certainly not less than one in magnitude). Thus, we have

$$s(\nu) + k_I l(\nu) > 0 \quad \text{for all } \nu, \qquad (62)$$

for any controller that satisfies all the specifications. Since the denominator is positive, we can multiply through by it, and express the linear fractional constraint (60) as

$$-(s(\nu) + k_I l(\nu)) \le a^T x + b \le s(\nu) + k_I l(\nu). \qquad (63)$$

This is a pair of linear inequalities in the variable x, since both $s(\nu)$ and $l(\nu)$ are linear functions of x.

With the notation (59) and taking into account (50), the controller design specifications for steady-state loop performance (31), (30), (34), (36), (37) can be presented in the form

$$\begin{aligned} -\bar{S}(\nu)^T x - \bar{H}(\nu)^T x &\le (d_0/u_0)\bar{K}(\nu)^T x \\ &\le \bar{S}(\nu)^T x + \bar{H}(\nu)^T x \quad (64) \\ -\bar{S}(\nu)^T x - \bar{H}(\nu)^T x &\le (d_0/e_0)\bar{S}(\nu)^T x \\ &\le \bar{S}(\nu)^T x + \bar{H}(\nu)^T x \quad (65) \\ -\bar{S}(\nu)^T x - \bar{H}(\nu)^T x &\le \delta_0 \bar{K}(\nu)^T x \\ &\le \bar{S}(\nu)^T x + \bar{H}(\nu)^T x \quad (66) \\ -\bar{S}(\nu)^T x - \bar{H}(\nu)^T x &\le \delta_C \bar{S}(\nu)^T x \\ &\le \bar{S}(\nu)^T x + \bar{H}(\nu)^T x \quad (67) \\ -\bar{S}(\nu)^T x - \bar{H}(\nu)^T x &\le \delta_S \le \bar{S}(\nu)^T x + \bar{H}(\nu)^T x \quad (68) \end{aligned}$$

where (65) is required to hold only within the assumed spatial bandwidth of the control, i.e., for $\nu \in \mathcal{B}$.

These specifications should be complemented by the loop dynamical response specifications (23) that can be presented in the form

$$\alpha_p \bar{H}(\nu)^T x + \beta_p \bar{S}(\nu)^T x + \gamma_p \le 0 \tag{69}$$
$$\alpha_o \bar{H}(\nu)^T x + \beta_o \bar{S}(\nu)^T x + \gamma_o \le 0 \tag{70}$$

where (69) is required to hold only in the control band, i.e., for $\nu \in \mathcal{B}$, and (70) is required to hold only out-of-band, for $\nu \notin \mathcal{B}$.

Finally, as the optimization objective we consider the spatial response decay. We require that the transfer function denominator $B(e^{i\nu}) = s(\nu) + k_I l(\nu)$ satisfies (41), where we will minimize t. In accordance with Proposition 1 the decay rate bound is guaranteed to improve for smaller t. Roughly speaking, we want the (dynamic) loop gain as uniform as possible for all spatial frequencies. We can achieve this goal by taking as objective

$$\phi(x) = \max_{\nu \in [0,2\pi]^n} |1 - \bar{S}(\nu)^T x - \bar{H}(\nu)^T x|. \tag{71}$$

Since this objective is the maximum of a family of convex functions (absolute values of linear functions), it is a convex function of x. If ϕ is small, then we can expect fast spatial decay of the closed-loop system response.

The overall design problem is a convex optimization problem:

$$\begin{array}{ll} \text{minimize} & \phi(x) \\ \text{subject to} & \text{linear inequalities (63) above, for each } \nu. \end{array}$$

The objective is given in (71), and the constraints are an infinite set of linear inequalities; specifically, ten per spatial frequency ν. (Such a problem is called *semi-infinite* since the constraints are indexed by the real number ν.)

Finally, we approximate the semi-infinite convex problem as an LP. We take a finite but sufficiently dense set of spatial frequencies, $\{\nu_1, \ldots, \nu_M\}$, and impose all of the linear inequalities at these frequencies only. This results in a large, but finite, number of linear inequalities. In practice, the number M of the frequency gridpoints required would depend on the highest spatial frequency in the representation (49) or (59) of the spatial operators (the largest tap delay in the FIR operators S and K). Of course, the frequency content of the system spatial operator $G(e^{i\nu})$ also needs to be taken into account. Refining the frequency grid always allows to achieve any prescribed accuracy of the solution.

Similarly, we approximate the objective by sampling over spatial frequencies:

$$\hat{\phi}(x) = \max_{\nu_i} |1 - \bar{S}(\nu_i)^T x - \bar{H}(\nu_i)^T x|.$$

This is a piecewise linear and convex function of x. We can in turn formulate this sampled problem as a linear program, by introducing a new variable γ, and adding the constraints

$$-\gamma \le 1 - \bar{S}(\nu_i)^T x - \bar{H}(\nu_i)^T x \le \gamma, \tag{72}$$

These constraints ensure that $\gamma \ge \hat{\phi}(x)$. Then we formulate the following linear program:

$$\begin{array}{ll} \text{minimize} & \gamma \\ \text{subject to} & -\gamma \le 1 - \bar{S}(\nu_i)^T x - \bar{H}(\nu_i)^T x \le \gamma, \\ & \text{linear inequalities (63) for each } \nu_i. \end{array} \tag{73}$$

In this problem, the objective and all constraints are linear, i.e., it is a linear program (LP).

The LP (73) has $2M_b + 3$ variables, and no more than $18M$ linear inequality constraints. (The exact number depends on the number of spatial frequency samples that fall in the control band $\mathcal{B}$.) It can be solved very quickly for typical problem sizes, e.g., several tens of variables, and several hundreds of constraints.

This method of synthesizing the spatial filters K and S can be used to tune the LTSI controller, by varying parameters in the specifications, such as the control band $\mathcal{B}$, the actuator limit u_0, the error limit e_0, and the constants related to various types of uncertainty, i.e., δ_0, δ_C, and δ_S. These parameters become the 'knobs' used by the control designer, that are varied to obtain adequate performance.

It should be clear from the discussion that many other specifications can also be included, and more complex specifications can also be handled by the method. As an example, we can impose a limit on loop gain that is a function of spatial frequency. In addition, we can impose limits on the magnitude of *any* steady-state closed-loop spatial transfer function, since every one will be linear fractional, with the same denominator as the ones considered.

V. SIMULATION EXAMPLE

As an example of applying the proposed feedback design approach, we consider a 3-D distributed estimation problem for a 2-D image evolving in time. The motivation for the problem below comes from estimating a slowly changing image from a series of noisy snapshots. Such images are common in industrial vision systems, medical diagnostics, nondestructive evaluation of materials. A closely related problem is of image deblurring.

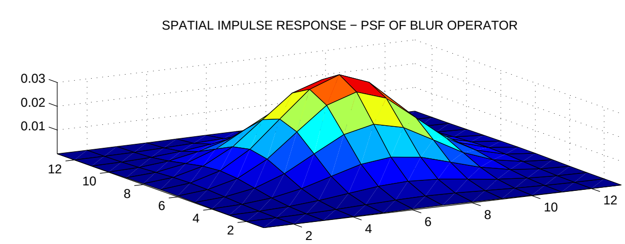

Fig. 3. Spatial response (point spread function) of the image blur operator

We assume a model of the form (15) where the 2-D FIR operator $G(\lambda)$ describes a Point Spread Function (PSF) of the imaging system. In practice, the PSF could be often determined by applying a point signal in a controlled experiment and observing the imaging system response. In this simulation example we postulate that $G(\lambda)$ is a known Gaussian blur operator

$$G(\lambda) = \sum_{n=-N_G}^{N_G} \sum_{k=-N_G}^{N_G} e^{-\frac{1}{2}(n^2+k^2)/a_G^2} \lambda_1^n \lambda_2^k, \qquad (74)$$

where the Gaussian width $a_G = 2$ and maximal delay of FIR operator $N_G = 6$ were assumed. The blur PSF operator $G(\lambda)$ is illustrated in Figure 3.

For the estimator design it was assumed that the dynamics are absent except the processing delay and a simple integral feedback of the form (11) is used such that

$$g(z^{-1}) = 1, \quad c(z^{-1}) = 1 \qquad (75)$$

The plant spatial operator $G(\lambda)$ in (74) has an 8-fold symmetry. Therefore the operators K and S in the controller (11) are also chosen to be 8-fold symmetric. These operators are represented in the form (55)–(57), (54) to yield

$$K(e^{i\nu_1}, e^{i\nu_2}) = \bar{K}(\nu_1, \nu_2)^T x, \quad S(e^{i\nu_1}, e^{i\nu_2}) = \bar{S}(\nu_1, \nu_2)^T x,$$
$$k_I G(e^{i\nu_1}, e^{i\nu_2}) K(e^{i\nu_1}, e^{i\nu_2}) = \bar{H}(\nu_1, \nu_2)^T x, \qquad (76)$$

where $\bar{K}$, $\bar{S}$, and $\bar{H}$ follow from (54), (56), (57).

Both operators K and S have $M = 5$ FIR taps on each side off the center, thus, with the 8-fold symmetry there are a total of $M_b + 1 = 1 + 2M + M(M-1)/2 = 21$ coefficients in each of the two FIR operators to be optimized.

The specifications for the estimator filter are formulated separately in the bandwidth domain (pass band) $\mathcal{B}_p$ and stop band $\mathcal{B}_s$. These domains were selected as

$$\begin{aligned} \mathcal{B}_p &= \{\nu_1, \nu_2 : |G(e^{i\nu_1}, e^{i\nu_2})| \geq 0.25\}, \\ \mathcal{B}_s &= \{\nu_1, \nu_2 : |G(e^{i\nu_1}, e^{i\nu_2})| \leq 0.1\} \end{aligned} \qquad (77)$$

We consider the following specifications for the estimator design.

Convergence (dynamical performance): For the estimator design, the specifications (22) have the form similar to (23). In-band (in the pass band), the estimate is required to converge quickly enough such that the filtered signal responds quickly to the change of the underlying image. On the opposite, dynamical low-pass filtering in the (spatial) stop band is required to be heavy enough. The filter time constant should be no less than a given value such that the dynamical noise is sufficiently reduced. These requirements can be expressed as

$$\left|1 - \bar{H}(\nu_1, \nu_2)^T x - \bar{S}(\nu_1, \nu_2)^T x\right| \leq \alpha_p, \quad \nu \in \mathcal{B}_p, \qquad (78)$$
$$\alpha_s \leq 1 - \bar{H}(\nu_1, \nu_2)^T x - \bar{S}(\nu_1, \nu_2)^T x \leq 1, \quad \nu \in \mathcal{B}_s, \qquad (79)$$

where $\alpha_p = 0.7$ and $\alpha_s = 0.85$ were assumed in the design example. This corresponds to the filter time constant being no more than 2.8 samples in band and no less than 6 samples in the stop band.

Steady-state Performance: The steady-state filter output can be expressed from (15), (18) as ($k_I = c(1) = 1$)

$$u = \frac{K(e^{i\nu_1}, e^{i\nu_2})}{S(e^{i\nu_1}, e^{i\nu_2}) + K(e^{i\nu_1}, e^{i\nu_2}) G(e^{i\nu_1}, e^{i\nu_2})} y,$$
$$\hat{y} = G(e^{i\nu_1}, e^{i\nu_2}) u \qquad (80)$$

The requirements to the steady state performance of the estimator follow from (80). The estimate $\hat{y}$ should be close to the signal y in band. This can be expressed as the transfer function relating $\hat{y}$ to y being close to unity in the pass band. To reject the noise, the signal $\hat{y}$ should be small in the stop band. The transfer function magnitude should be small.

Assume a bound v_0 on the magnitude of the source image v and a bound d_0 on the magnitude of the disturbance d. By substituting (76) into (80) and making the estimates similar to (34), (36) we obtain the steady state performance requirements in the form

$$\begin{aligned} \bar{H}(\nu_1, \nu_2)^T x &\leq (1+E) \cdot \left(\bar{S}(\nu_1, \nu_2)^T x + \bar{H}(\nu_1, \nu_2)^T x\right), \\ \bar{H}(\nu_1, \nu_2)^T x &\geq (1-E) \cdot \left(\bar{S}(\nu_1, \nu_2)^T x + \bar{H}(\nu_1, \nu_2)^T x\right), \\ & \quad \text{for } \{\nu_1, \nu_2\} \in \mathcal{B}_p \qquad (81) \\ \left|\bar{H}(\nu_1, \nu_2)^T x\right| &\leq V_1 \cdot \left(\bar{S}(\nu_1, \nu_2)^T x + \bar{H}(\nu_1, \nu_2)^T x\right), \\ & \quad \text{for } \{\nu_1, \nu_2\} \in \mathcal{B}_s \qquad (82) \end{aligned}$$

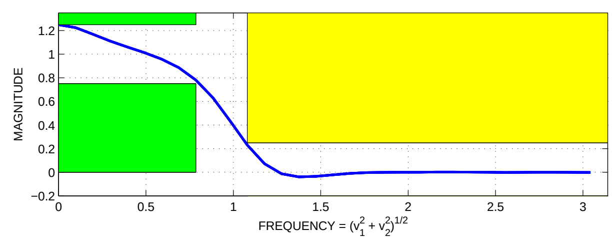

Fig. 4. Filter specification requirements: 1-D cross section of the requirements in the 2-D domain of spatial frequencies.

In the design example we assumed $E = 0.25$ and $V_1 = 0.25$. The design requirements are illustrated in Figure 4. They can be expressed as as linear inequalities in the form similar to (64), (65).

The requirements (81), (82) need to be complemented by the requirement of the bounded amplification of the input signal y when computing the intermediate estimate u in (80). Unless this requirement is in place, the large intermediate signal u could lead to instability caused by the boundary effects.

$$V_0 \left|\bar{K}(\nu_1, \nu_2)^T x\right| \leq \bar{S}(\nu_1, \nu_2)^T x + \bar{H}(\nu_1, \nu_2)^T x, \qquad (83)$$

where $\{\nu_1, \nu_2\} \in [0,\ 2\pi]^2$. In the design example, $V_0 = 3$ was assumed.

Spatial response decay: Finally, as the optimization objective we will take the decay rate of the steady state closed-loop response (boundary layer width). This objective can be expressed in the following form that is similar to (71) with a potential scaling factor difference.

$$-1 \leq \gamma_1 \leq 1 - \bar{S}(\nu_1, \nu_2)^T x - \bar{H}(\nu_1, \nu_2)^T x \leq \gamma_2 \leq 1 \qquad (84)$$
$$\gamma_2 - \gamma_1 \to \min$$

A. Estimator implementation and simulation results

The formulated linear inequalities and the optimization objective (84) were integrated together to yield an optimization problem with respect to the parameter vector $x = [p_S^T \ p_K^T \ q_1 \ q_2]^T$, where p_S and p_K each contain 21 independent coefficients of the respective FIR operators S and

K to be optimized, 44 coefficients at all in the parameter vector x (58). The controller tuning problem was cast as an LP problem with respect to x, as described above, with spatial frequency sampled at $64 \times 64 = 4096$ points uniformly spaced in the spatial frequency domain $[0, 2\pi] \times [0, 2\pi]$. The problem was solved using the LINPROG medium-scale LP solver from Matlab® Optimization Toolbox. The designed spatial FIR operators K and S of the filter are illustrated in Figure 5.

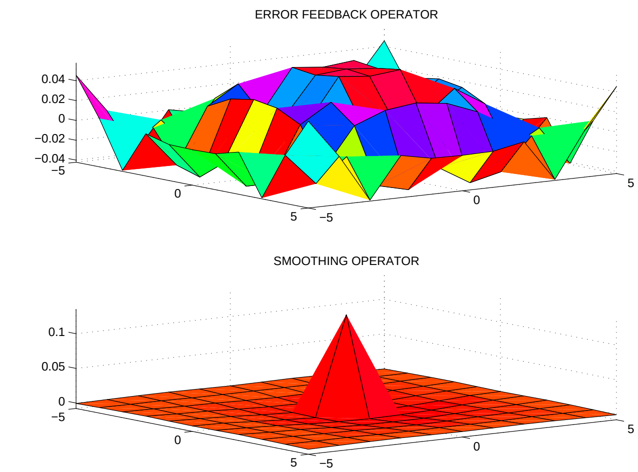

Fig. 5. Designed spatial FIR operator for the 3-D estimator filter. Feedback operator K - upper plot, smoothing operator S - lower plot.

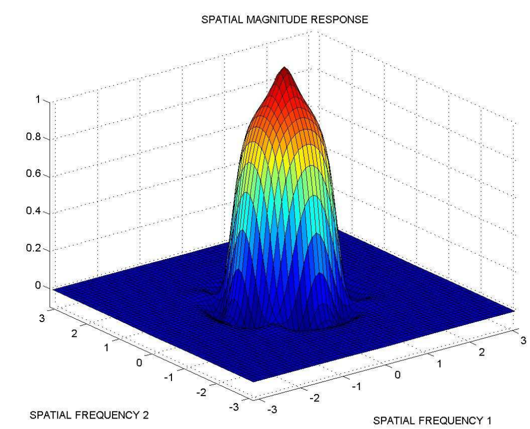

Fig. 6. Filter magnitude response function for steady state ($w = 0$).

The transfer function magnitude for the designed filter at steady state (at $w = 0$) is displayed in Figure 6. Figure 7 shows the time constant of the filter depending on the spatial frequency

$$\tau(\nu_1, \nu_2) = \frac{-1}{\log\left(1 - K(e^{i\nu_1}, e^{i\nu_2})G(e^{i\nu_1}, e^{i\nu_2}) - S(e^{i\nu_1}, e^{i\nu_2})\right)}.$$

The steady-state spatial impulse response of the filter is illustrated in Figure 8. It decays in 5-8 samples off the centers. This shows how far the influence of the boundary conditions would extend onto the spatial domain of the filtered signal.

The designed filter was applied to a noisy image sequence generated as follows. The spatial domain of 40 × 100 pixels

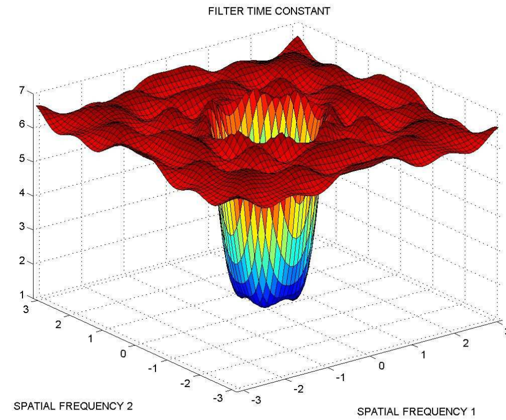

Fig. 7. Filter time constant $\tau(\nu_1, \nu_2)$ depending on the spatial mode frequencies.

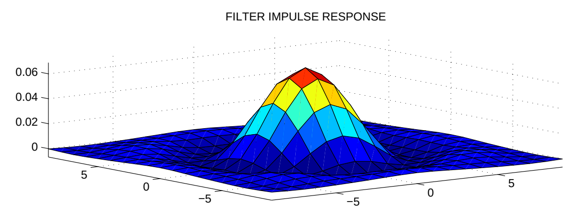

Fig. 8. Steady state impulse response of the closed loop.

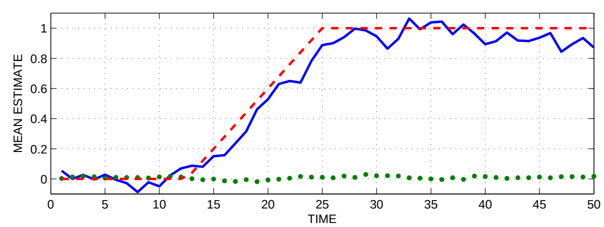

Fig. 9. Correlation between the applied and estimated signal (solid line). Time series of the applied signal amplitude (dashed line)

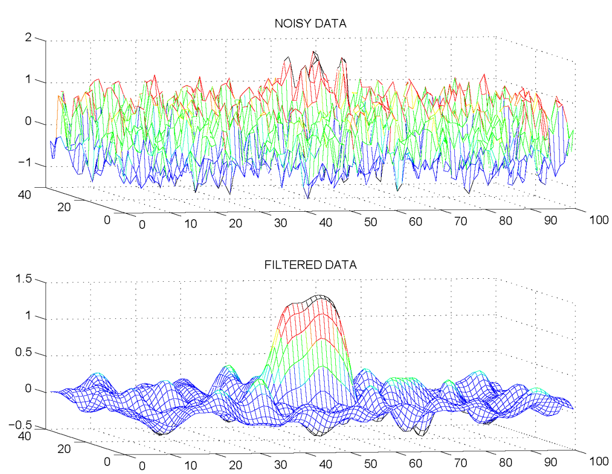

Fig. 10. Noisy data snapshot (upper plot). Filtered data snapshot (lower plot)

was considered with the source signal v being zero in the most of the domain, except an ellipse with the main axes of 8 (along x_1) and 20 (along x_2) in the center of the domain. The signal v was ramped up from zero to unity in 12 time steps uniformly inside the ellipse. The signal v was distorted by an additive (pseudo-)random noise uniformly distributed in the interval $[-2, 2]$ and uncorrelated in time and space. The noisy signal was then smoothed (blurred) by applying a scaled Blackman window (a FIR operator $[0.2024 \;\; 0.5952 \;\; 0.2024]$) along each of the directions x_1 and x_2. The generated 3-D signal was used as an input to the designed filter. In practice the blur might be not known accurately, which is reflected by the blur in the simulation being differs from what is assumed in the filter design. The simulation results are illustrated in Figures 9 and 10.

The time dependency of the filtered data can be illustrated by taking average values inside the central ellipse and outside of it. The time series for these average values are illustrated in Figure 9. The plot also show the magnitude of the source signal inside the ellipse (it is zero outside). The time series for the filtered signal follows the time dependencies for the source very closely. This means that despite the significant improvement in signal-to noise ratio, the filtering delay is insignificant.

The 2-D slices of the signals in Figure 10 is taken at time 50 well afer the end of the ramp. The raw, noisy, 2-D data in the upper plot makes the source signal v hardly visible. In the filtered data, (the lower plot) the signal is significantly (factor 3-5) above the noise.

VI. Conclusions

The LP optimization scheme for distributed controller tuning has been proposed. A straightforward design approach implements many engineering specifications in natural framework. It was demonstrated through simulation that the proposed method allows achieving very good quality of control and estimation in difficult distributed system problems.

References

[1] Abraham, R. and Lunze, J. "Modelling and decentralized control of a multizone crystal growth furnace," *Int. J. Robust and Nonlinear Control*, Vol.2, 1992, pp. 107–122.

[2] Bamieh, B., Paganini, F., and Dahleh, M. "Distributed control of spatially-invariant systems," *IEEE Trans. on Automatic. Contr.*, Vol. 47, No. 7, July 2002. pp. 1091–1107.

[3] Beck, C.L. and Doyle, J. and Glover, K. "Model reduction of multidimensional and uncertain systems," *IEEE Trans. on Automatic Control*, Vol. 41, No. 10, 1996, pp. 1466–1477.

[4] Bose, N.K. *Applied Multidimensional Systems Theory*, Van Nostrand Reynhold, 1982

[5] Boyd, S. and Barratt, C. *Linear Controller Design: Limits of Performance*, Prentice-Hall, 1991

[6] Boyd, S. and Vandenberghe, L. *Convex Optimization*, Cambridge University Press, 2004.

[7] Brockett, R.W. and Willems, J.L. "Discretized partial differential equations: examples of control systems defined on modules," *Automatica*, Vol. 10, 1974, pp. 507–515.

[8] Chottera, A. and Jullien, G. "Design of two-dimensional recursive digital filters using linear programming," *IEEE Trans. on Circuits and Systems*, Vol. 29, No. 12, 1982, pp. 817–826.

[9] Coulombe, S. and Dubois, E. "Linear phase and symmetries for multidimensional FIR filters over lattices," *IEEE Trans. Circuits Syst. II, Analog Digit. Signal Process.*, Vol. 45, Apr. 1998, pp. 473-481.

[10] D'Andrea, R. "Linear matrix inequaly approach to decentralized control of distributed parameter systems," *American Control Conf.*, Philadelphia, PA, pp.1350–1354, June 1998

[11] D'Andrea, R., and Dullerud, G.E., "Distributed control for spatially interconnected systems," *IEEE Trans. on Automatic Control*, Vol. 48, No. 9, 2003, pp. 1478–1495.

[12] De Castro, G. A. and Paganini, F. "Convex synthesis of localized controllers for spatially invariant systems," *Automatica*, Vol. 38, No. 3, 2002, p.445-450.

[13] Special Issue on Control of Industrial Spatially Distributed Processes, Eds. Dochain, D., Dumont, G., Gorinevsky, D., and Ogunnaike, T., *IEEE Trans. on Control Systems Technology,* Vol. 11, No. 5, 2003.

[14] Dudgeon, D.E. and Mersereau, R.M. *Multidimensional Digital Signal Processing*, Prentice-Hall, 1984.

[15] Duncan, S. R. , "The design of robust cross-directional control systems for paper making," *American Control Conf.*, pp. 1800–1805, Seattle , WA, 1995.

[16] Gorinevsky, D. "Loop-shaping for iterative control of batch processes," *IEEE Control Systems Magazine*, Vol. 22, No. 6, 2002, pp. 55–65.

[17] Gorinevsky, D. and Boyd, S. "Optimization-based design and implementation of multi-dimensional zero-phase IIR filters," *IEEE Trans. on Circuits and Systems - I*, Vol. 53, No. 2, 2006, pp. 372-386

[18] Gorinevsky, D., Boyd, S., and Stein, G. "Optimization-based tuning of low-bandwidth control in spatially distributed systems," *American Control Conference*, Vol. 3, pp. 2658–2663, Denver, CO, June 2003.

[19] Gorinevsky, D. and Gheorghe, C. "Identification tool for cross-directional processes," *IEEE Trans. on Control Systems Technology*, Vol. 11, No. 5, 2003, pp. 629–640.

[20] Gorinevsky, D. and Gordon, G. "Spatio-temporal filter for structural health monitoring," *American Control Conf.,* Minneapolis, MN, June 2006

[21] Gorinevsky, D. and Stein, G. "Structured uncertainty analysis of robust stability for multidimensional array systems," *IEEE Trans. on Automatic Control*, Vol. 48, No. 8, 2003, pp. 1557–1568.

[22] Gorinevsky, D., Hyde, T., and Cabuz, C. "Distributed shape control of lightweight space reflector structure," *IEEE Conference on Decision and Control*, Vol. 4, pp.3850–3855, Orlando, FL, December 2001,

[23] Heaven, E.M., Jonsson, I.M., Kean, T.M., Manness, M.A., and Vyse, R.N. "Recent advances in cross machine profile control," *IEEE Control Syst. Mag.*, vol. 14, no. 5, Oct. 1994.

[24] Langbort, C. and D'Andrea, R. "Distributed control of spatially reversible interconnected systems with boundary conditions," *SIAM Journal of Control and Optimization*, vol. 44, no. 1, 2005, pp. 1–28.

[25] Lim, J.S. *Two-Dimensional Signal and Image Processing*, Prentice Hall, 1990.

[26] Mijanovic, S., Stewart, G.E., Dumont, G.E., and Davies, M.S. "Design of an industrial distributed controller near spatial domain boundaries," *American Control Conference*, Vol. 4, pages 3574–3580, Boston, MA, June 30-July 3, 2004.

[27] Oppenheim, A.V., Schafer, R.W., and Buck, J.R. *Discrete-Time Signal Processing*, Prentice Hall, 1999 A recursive information flow system for distributed control arrays

[28] Paganini, F., "A recursive information flow system for distributed control arrays," *American Control Conf.*, Vol. 6, pages 3821–3825, San Diego, CA, 2-4 June, 1999.

[29] Pitas, J. and Venetsanopoulos, A. "The use of symmetrics in the design of multidimensional digital filters," *IEEE Trans. on Circuits and Systems*, Vol. 33, No. 9, 1986, pp. 863–873.

[30] Rabiner, L., Graham, N., and Helms, H. "Linear programming design of IIR digital filters with arbitrary magnitude function," *IEEE Trans. on Acoustics, Speech, and Signal Processing* , Vol. 22, No. 2, 1974, pp. 117 - 123.

[31] Stein, G. and Gorinevsky, D. "Design of surface shape control for large two-dimensional arrays," *IEEE Trans. on Control Systems Technology* vol. 13, no. 3, pp. 422 - 433, May 2005.

[32] Stewart, G.E., Gorinevsky, D., and Dumont, G.A. "Feedback controller design for a spatially-distributed system: The paper machine problem," *IEEE Trans. on Control Systems Technology*, Vol. 11, No. 5, 2003, pp. 612–628.

[33] Stewart, G.E., Gorinevsky, D., and Dumont, G.A. "Two-dimensional loop shaping," *Automatica*, Vol. 39, No. 5, 2003, pp. 779-792.

[34] Tikhonov, A.N., and Arsenin, V.Ya. *Solutions of Ill-Posed Problems*. Halsted Press, Washington, 1977.

[35] Wu, S.-P., Boyd, S., and Vandenberghe, L. "FIR Filter Design via Spectral Factorization and Convex Optimization," *Applied and Computational Control, Signals and Circuits*, Ch. 2, pp. 51–81, Birkhauser, 1997

PLACE
PHOTO
HERE

Dimitry Gorinevsky (M'91–SM'98–F'06) received a Ph.D. degree from department of mechanics and mathematics of Moscow (Lomonosov) University, in 1986, and a M.Sc. in aerospace engineering from the Moscow Institute of Physics and Technology, in 1982.

He is a Consulting Professor of Electrical Engineering at Stanford University and an independent consultant to NASA. He worked for Honeywell for 10 years. Prior to that, he held research, engineering, and academic positions in Moscow, Russia; Munich, Germany; Toronto and Vancouver, Canada. His interests are in decision and control systems applications across many industries. He has authored a book, more than 140 reviewed technical papers and a dozen patents. Dr. Gorinevsky is an Associate Editor of IEEE Transactions on Control Systems Technology. He is a recipient of Control Systems Technology Award, 2002, and Transactions on Control Systems Technology Outstanding Paper Award, 2004, of the IEEE Control Systems Society.

PLACE
PHOTO
HERE

Stephen Boyd (S'82–M'85–SM'97–F'98) received the A.B. degree in Mathematics from Harvard University in 1980, and the Ph.D. in Electrical Engineering and Computer Science from the University of California, Berkeley, in 1985.

He is currently the Samsung Professor of Engineering, and Professor of Electrical Engineering in the Information Systems Laboratory at Stanford University. His current research focus is on convex optimization applications in control, signal processing, and circuit design.

PLACE
PHOTO
HERE

Gunter Stein (S'66–M'69–F'85) received a PhD in Electrical Engineering from Purdue University in 1969.

He is a Chief Scientist (ret) of Honeywell Technology Center (now Honeywell Labs). His technical specialization is in systems and control, particularly aircraft flight controls (fighters, transports, and experimental vehicles), spacecraft attitude and orbit controls, and navigation systems for strategic, tactical, and commercial applications. From 1977 to 1997, Dr. Stein also served as Adjunct Professor in EE and CS at MIT, teaching control systems theory and design. He is also active in the development of computer aids for control system design. Dr. Stein was elected Fellow of the IEEE in 1985, was awarded the IEEE Control System Society's first Hendrick W. Bode Prize in 1989, was elected to the National Academy of Engineering in 1994, and was awarded the IFAC's Nathaniel Nichols Prize in 1999.